

## Inertial effects in thermoacoustic subcritical bifurcation

Giacomo Bonciolini<sup>\*1</sup>, Edouard Boujo<sup>1</sup> and Nicolas Noiray<sup>1</sup>

<sup>1</sup>CAPS Laboratory, MAVT department ETH Zürich, 8092, Zurich, Switzerland

**Summary.** In combustion chambers, thermoacoustic coupling can lead to high acoustic levels, which are harmful for the system mechanical integrity. In this work, this complex phenomenon physics is reduced to a low-order phenomenological model, represented by a non-linear noise-driven oscillator. This model mimics the main aspects of the dynamics observed in gas turbine combustors, aero or rocket engines. In particular, this model is able to reproduce the situation in which a control parameter is changed, leading to a subcritical bifurcation of one of the thermoacoustic modes. The main purpose of this paper is to investigate transient inertial effects when the bifurcation bistable region is crossed in a finite time.

### Introduction

Thermoacoustic instabilities are experienced in most of the constant pressure combustion systems. Caused by a constructive interaction between acoustic pressure and heat release rate fluctuations, this phenomenon can produce a high-amplitude limit cycles. These can damage the combustor and therefore prevent the machine to be operated at optimal conditions [1]. The stability of the system is a function of many different physical parameters, such as operating pressure, inlet temperature or fuel/air ratio. In some cases, the system displays a subcritical bifurcation when these parameters are varied, going suddenly from a “quiet” regime to a high-amplitude limit cycle [2]. In the operating points lying between the critical and the Hopf points, a bistable regime establishes, due to the strong turbulence-induced heat release fluctuations, which act as a stochastic forcing. An example is provided in fig. 1, where a lab-scale combustor dynamic pressure  $p$  and amplitude  $A$  time traces are presented, together with their statistics, at three different operating points. One can observe how the Probability Density Function (PDF) of the amplitude  $P(A)$  changes accordingly, presenting two distinct maxima in the second case.

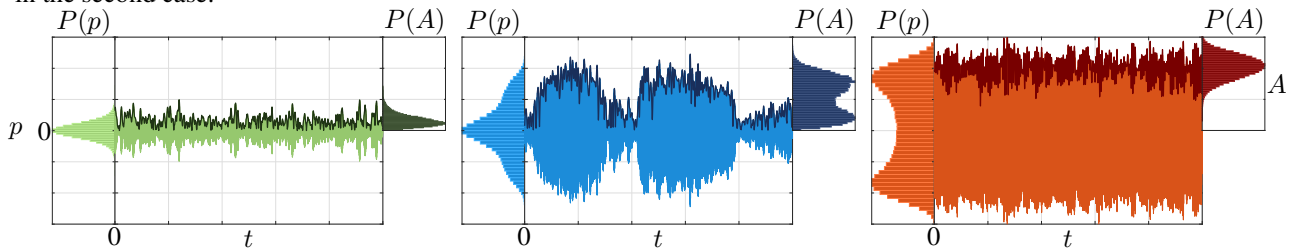


Figure 1: Lab-scale combustor dynamic pressure  $p(t)$  (light) and amplitude  $A(t)$  (dark) signals and relative statistics at three different operating points. Left: stable operation, Center: bistable, Right: high amplitude limit cycle.

### Non-linear oscillator model

A simple phenomenological model of a thermoacoustic system with subcritical bifurcation is provided by the nonlinear oscillator:

$$\ddot{p} + \omega_0^2 p = [2\nu + \kappa p^2 - \gamma p^4] \dot{p} + \xi, \quad (1)$$

where  $\omega_0$  is the angular frequency,  $\nu$  the oscillation linear growth rate,  $\kappa$  and  $\gamma$  two constants that set the non-linear response of the oscillator. The term  $\xi$  is a white noise forcing of intensity  $\Gamma$  that models non-coherent turbulence-induced heat release rate fluctuations. The RHS of this equation is in practice smaller than the LHS, hence one can assume  $p(t) = A(t) \cos(\omega_0 t + \phi(t))$  and derive a Langevin equation for the slowly-varying amplitude  $A(t)$ :

$$\dot{A} = A \left( \nu + \frac{\kappa}{8} A^2 - \frac{\gamma}{16} A^4 \right) + \frac{\Gamma}{4\omega_0^2 A} + \mu = \mathcal{F}(A) + \mu, \quad \text{with} \quad \langle \mu \mu_\tau \rangle = \frac{\Gamma}{2\omega_0^2} \delta(\tau), \quad (2)$$

where  $\mathcal{F}(A) = -dV/dA$ , i.e. the derivative of a potential. The variation in time of the PDF for the amplitude  $P(A, t)$  is described by the Fokker-Planck equation (FPE):

$$\frac{\partial}{\partial t} P(A, t) = -\frac{\partial}{\partial A} [\mathcal{F}(A) P(A, t)] + \frac{\Gamma}{4\omega_0^2} \frac{\partial^2}{\partial A^2} P(A, t), \quad (3)$$

which then gives for  $t \rightarrow \infty$  the stationary PDF  $P_\infty(A) = \mathcal{N} \exp[-4\omega_0^2 V(A)/\Gamma]$ . In fig. 2a, the map of the stationary PDF is plotted in a bifurcation diagram fashion, as a function of the linear growth rate  $\nu$ . One can observe the bistability region, bounded between  $\nu_1$  and  $\nu_2$ . This corresponds to the range of  $\nu$  that generates a potential  $V(A)$  featuring two minima, i.e. two potential wells separated by a potential barrier at  $A = A_B(\nu)$ .

<sup>\*</sup>Corresponding author: giacomob@ethz.ch

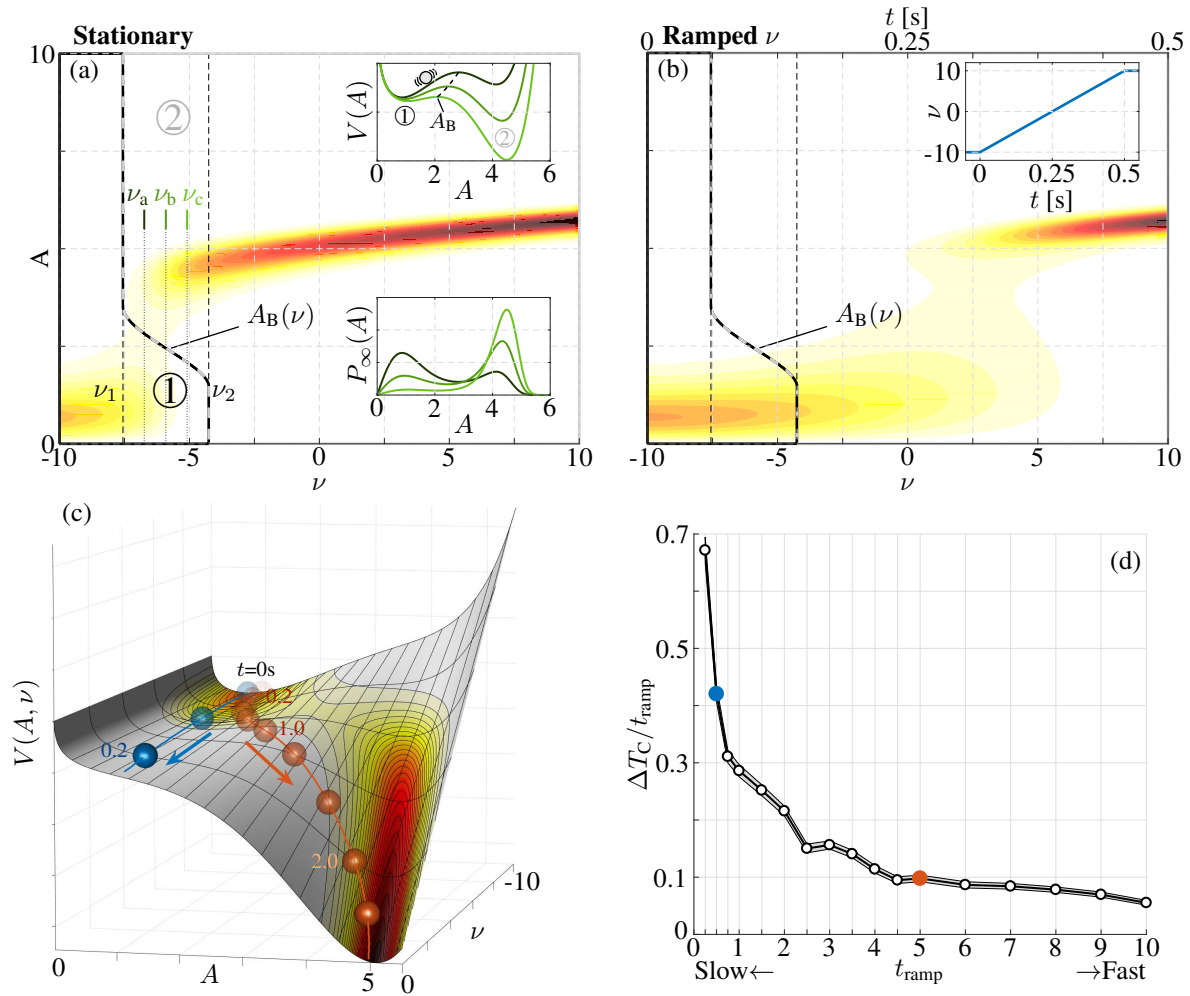


Figure 2: Low-order model description of the bifurcation process. a) Stationary PDF map  $P_\infty(A, \nu)$ , with the two potential wells ① and ②, separated by the boundary amplitude  $A_B(\nu)$ . In the insets the potential  $V$  and the PDF  $P_\infty$ , for three selected points ( $\nu_a, \nu_b, \nu_c$ ) in the bistable region. b) Solution of the unsteady FPE for  $P(A, \nu(t))$ , with the growth rate  $\nu$  varying linearly in  $t_{\text{ramp}} = 0.5\text{s}$ . c) Mechanical analogy of the process, described as a ball rolling on the potential surface  $V(A, \nu)$ : ball mean path for two ramping times  $t_{\text{ramp}} = 0.5\text{s}$  (blue) and  $t_{\text{ramp}} = 5\text{s}$  (red). d) Relative bifurcation delay  $\Delta T_C / t_{\text{ramp}}$ , as a function of the ramp time  $t_{\text{ramp}}$ . Colored points correspond to the two cases in c).

### Unsteady Fokker-Planck equation and mean first-passage

To unveil the oscillator dynamics peculiarities, time domain simulation of eq. (1) and numerical solution of eq. (3) are performed with  $\nu$  varying linearly in time. The two approaches are in very good agreement. The solution of the FPE is presented in fig. 2b. A delay in the transition from the quiet regime to the loud one is observed: the oscillations remain bounded for some time in a range of small amplitudes even though, in the stationary case, these points would be unstable. Other phenomena, like hysteresis when ramping from high to low  $\nu$ , are correctly captured by simulations and FPE.

To quantify the delay in transition from quiet to loud regime, the Mean First Passage Time is considered. In the bistable range, i.e.  $\nu \in ]\nu_1; \nu_2[$ , this is defined as the average time  $T_{\text{MFP}}(\nu)$  needed for the state to reach the high-amplitude potential well for the first time. In case of a ramping, the potential barrier between the two wells moves in time ( $A_B(\nu(t))$ ), and for  $\nu > \nu_2$  only the high-amplitude well remains. Even when the low-amplitude well has disappeared, the system does not readily transit to the stable limit cycle regime. In fig. 2c this phenomenon is presented via a mechanical analogy: the state is a ball rolling on the potential surface. When the ball is fast (blue), its inertia makes it roll straighter than the slow (red) ball, which falls in the high-amplitude well right after this appears. The average time  $T_C$  needed to cross the moving potential barrier  $A_B(t)$  is estimated via simulations of the process, and a relative crossing delay  $\Delta T_C = T_C - T_{\text{MFP}}(\nu(T_C))$  is computed. Figure 2d shows how the inertial effects have a stronger relevance for fast ramping, leading to a higher relative delay. This fact has a practical impact when one is mapping the operative points of a new combustion system: excessive ramp speeds cause the system to jump later to the limit cycle and therefore with higher amplitude, and a longer time is then needed to bring it back to a safe operating condition.

### References

- [1] Poinsot T. (2016), Prediction and control of combustion instabilities in real engines, *Proceedings of the Combustion Institute*.
- [2] Berglund N. and Gentz B. (2001), Pathwise description of dynamic pitchfork bifurcations with additive noise, *Probab. Theory Relat. Fields* 122.